Scientific paper

Hydrogenation of Unsaturated Carbonyl Compounds on non-Calcined LDHs. I. Synthesis and Characterization of ZnNiCuAl Hydrotalcite-like Materials

Brindusa Dragoi,[1,*] Adrian Ungureanu,[1] Alexandru Chirieac,[1] Vasile Hulea,[2] and Emil Dumitriu[1]

[1] *Faculty of Chemical Engineering and Environmental Protection, Technical University of Iasi, Department of Organic and Biochemical Engineering, Bd. D. Mangeron, 71A, 700050, Romania*

[2] *Ecole Nationale Supérieure de Chimie de Montpellier, 8 Rue de l'Ecole Normale, 34296 Montpellier CEDEX 5, France*

** Corresponding author: E-mail: bdragoi@ch.tuiasi.ro*

Received: 16-10-2009

Abstract

Several Zn/Ni/Cu/Al layered double hydroxides (LDH) with variable Ni/Cu ratios but constant Zn/Al, as well as M^{2+}/M^{3+} ratios, were synthesized by coprecipitation method with CO_3^{2-} as compensating anion. The main goal of the study was to investigate the influence of the catalysts composition, especially Ni/Cu ratio, on the physical and catalytic properties of these materials. The XRD results show that all the LDHs samples are well crystallized and contain only pure phases. Moreover, the spectral techniques (FT-IR and DR-UV-VIS) indicated that both Ni and Cu species are present in the brucite-like layers of LDHs. The shape of the nitrogen physisorption isotherms obtained at –196 °C indicates a predominantly mesoporous materials; the surface areas and pore volumes are in the specific ranges between 37–86 $m^2.g^{-1}$ and 0.31–0.75 $cm^3.g^{-1}$, respectively. Three characteristic weight losses between 30 and 400 °C are identified by TG analysis for the hydrotalcite-like materials synthesized in this study. Moreover, an influence of the Ni/Cu ratios on the amount of the physisorbed water was noticed. The preliminary catalytic test revealed unusual catalytic properties of the non-calcined samples in the liquid phase hydrogenation of *trans*-cinnamaldehyde.

Keywords: Layered double hydroxides, synthesis, characterization, hydrogenation, cinnamaldehyde.

1. Introduction

A contribution to the implementation of green and sustainable chemistry in industrial applications could be the development of multifunctional heterogeneous catalysts which possess various catalytic functions at the surface, such as acid, base and redox sites. Among them, layered double hydroxides (LDH), also called anionic clays or hydrotalcite-like compounds, have recently received much attention in view of their potential as adsorbents, anion exchangers, and the most importantly as catalysts. These compounds are represented by the formula $(M_{(1-x)}^{2+}M_x^{3+}(OH)_2)^{x+}(A_{x/n}^{n-}{}_m H_2O)^{x-}$, where the divalent ion may be Mg^{2+}, Cu^{2+}, Zn^{2+}, Ni^{2+}, and the trivalent ion Al^{3+}, Fe^{3+}, Cr^{3+}. The compensating anions may be CO_3^{2-}, OH^-, SO_4^{2-}, NO_3^-, Cl^-, and "x" can have values between 0.17 and 0.33. As concerns the structure, such materials have an alternating layered structure with positively charged brucite-like layers ($M^{2+}M^{3+}(OH)$), where M^{2+} cations are substituted by M^{3+} cations, and interlayers containing the charge balancing anions and water molecules.[1–3] Usually, the catalytic applications were mainly reported on the homogeneous mixed oxides resulted by the calcination of LDHs and only few studies on the non-calcined materials.[4] Polymerization of alkene oxides, aldol condensation of aldehydes and ketones, and methane or hydrocarbons steam reforming, methanation, methanol synthesis, and higher alcohols or hydrocarbon synthesis (Fischer-Tropsch), the selective hydrogenation of maleic anhydride to γ–butyrolactone, the partial oxidation of methane to synthesis gas and the selective catalytic reduction (SCR) of NO by ammonia cover only a part of their catalytic applications.[5]

The chemoselective hydrogenation of unsaturated carbonyl compounds is the focus of special interest since

this is often a key step in the preparation of various fine chemicals.[6] The most challenging class of these chemoselective hydrogenations is the reduction of α,β–unsaturated aldehydes to allylic alcohols. This is also the case of the selective trans-cinnamaldehyde (CNA) hydrogenation to cinnamyl alcohol (CNOL), both substances being of practical importance due to their applications in the fine chemicals and perfume industries.[7]

The catalytic hydrogenation of cinnamaldehyde to the corresponding allylic alcohol (CNOL) has an obstacle: from the thermodynamical data it was established that the carbon-oxygen double bond (the carbonyl group, >C=O) is more difficult to be hydrogenated than the carbon-carbon double bond (olefin group, >C=C<).[8] At the same time the reaction might give a broad spectrum of by-products originating from undesired aromatic ring hydrogenation, hydrogenolytic and condensation reactions and even the isomerisation of CNOL to CNA. The best results for such selective hydrogenations were obtained using noble metals based catalysts but in the view of sustainable chemistry it is a true challenge to replace them by cheaper catalysts based on non-noble metals.[9,10] The use of non-noble metals for selectively hydrogenating α,β-unsaturated aldehydes has been reported in several papers. Nickel and copper based oxides resulted from LDH precursors have shown interesting characteristics of chemo-, regio-, and stereoselectivity for hydrogenation reactions, [11–13] but do not exhibit a high selectivity to form unsaturated alcohols from α,β-unsaturated aldehydes.[11–15] Attempts for improving the intrinsic catalytic properties of copper and nickel could take into account the formation of bimetallic Ni–Cu particles, the interactions between metal and support, and interactions of the *d* orbitals.

In this work, we prepared a set of catalysts containing various amounts of Cu and Ni atoms homogeneously highly dispersed in a lattice of ZnAl LDH (Zn/Al is kept constant and equal to 1/1) by coprecipitation method at low supersaturation. The originality of this study consists in exploring the catalytic performance of these materials (as-synthesized LDHs) in the liquid phase hydrogenation of cinnamaldehyde (3-phenyl-2-propenal, CNA) as such namely, by avoiding the calcination step which leads to the formation of mixed oxides, which is an energy and time consuming step. Also, by calcination at high temperatures new crystalline phases like spinels could be formed, and often such phases proved non-suitable catalytic behavior.

2. Experimental

2. 1. Synthesis of LDHs

A series of NiCuZnAl hydrotalcites with variable Ni to Cu ratios, but constant M^{2+}/M^{3+} ratio in all the samples ($M^{2+}/M^{3+} = 2$), was prepared by coprecipitation under low supersaturation method. An aqueous solution containing a mixture of MSO_4 hydrate (M = Zn, Ni, Cu) and $Al_2(SO_4)_3 18H_2O$ as metal sources and a mixture of NaOH (1.6 M solution) and Na_2CO_3 (0.8 M solution) as precipitants were simultaneously added at a flow rate of 0.7 $ml.min^{-1}$ under vigorous stirring and constant temperature (25 °C) and pH = 8.0. The precipitate obtained was aged overnight at the same temperature and vigorous stirring. Then, the precipitate was filtered under vacuum and washed with large amounts of distilled water until the washings were free from Na^+ ions. The solids were dried at 30 °C at constant weight. The samples were labeled according to the elements compositions and codes "xy" indicate the atomic ratio between Ni and Cu cations.

2. 2. Characterization

The resulting solids were systematically characterized by powder XRD, nitrogen physisorption, FT-IR, DR-UV-VIS and thermogravimetry.

XRD measurements were performed using a Bruker D5000 apparatus with monochormatic CuKα radiation (λ = 1,541Å wavelength) at room temperature. All patterns were recorded over the 2θ range from 3 to 50° with a step 0,100°. The crystallites size of LDHs samples were calculated by using Scherrer equation: $D_{hkl} = \lambda/\beta\cos\theta$, where λ = incident ray wavelength (0.15406 nm); β = peak width at half height (rad), θ = Bragg angle.

Nitrogen physisorption was carried out on a Autosorb MP-1 (Quantachrome) at –196 °C. Surface area, pore volume and pores size distribution were obtained from the corresponding isotherms using the conventional methods of BET, de Boer and BJH.

Infrared spectra were collected on a Scimitar FTS 2000 (Digilab) between 400 and 4000 cm^{-1}, 50 acquisitions per spectrum and a resolution of 4 cm^{-1}. The samples were used as pellets formed from a mixture of 99 mg KBr and 1 mg of LDH sample.

Diffuse reflectance UV–visible (UV–vis) spectra were recorded on a Shimadzu UV-2450 spectrometer equipped with an integrating sphere unit (ISR-2200). The spectra were collected at 200–800 nm with $BaSO_4$ as reference.

Thermogravimetric analysis was performed on computer coupled Q-derivatograph (MOM). The samples were analyzed in the temperature range between 30–600 °C with a heating rate of 10 °C·min^{-1}. All measurements were performed in air.

2. 3. Catalytic Test: Hydrogenation of Trans-cinnamaldehyde

For each test, the non-calcined catalyst was reduced in a hydrogen flow (1 $L.h^{-1}$) at 150 °C for 2 h (heating rate of 6 °C·min^{-1}). The test was carried out at atmospheric pressure in a three neck glass reactor equipped with reflux condenser and magnetic stirring (900 rpm) under the following conditions: 1 ml of reagent (7.94×10^{-3} mol),

25 ml of propylene carbonate as solvent, and 0.264 g of catalyst, hydrogen flow 1 L.h^{-1}, and constant temperature of reaction 150 °C.

The samples were periodically taken off and analyzed by an HP 5890 Series gas-chromatograph, which is equiped with a capillary column DB – 5 (25 m × 0,20 mm × 0,33 μm) and a flame ionization detector, with the following temperature program: initial temperature of 150 °C (1 min), and heating (15 °C·min^{-1}) until 270 °C.

3. Results and Discussion

3. 1. Physico-chemical Characterization

The crystalline structure and lattice parameters were investigated by powder X-ray diffraction measurements. As it can be seen in Figure 1, the XRD diffraction patterns for carbonate-LDHs show symmetrical reflections for (003), (006), (110), (113) planes and broad asymmetrical peaks for (012), (015), (018) planes. All these peaks are characteristics of crystalline single hydrotalcite-like phase.[1] This also indicates that Ni^{2+} and Cu^{2+} cations are isomorphously substituted in the brucite like layers.

Generally, the lattice parameters of LDH crystals are calculated by indexing the peaks under hexagonal crystal system and 3R symmetry, the parameter "*a*" corresponding to the cation–cation distance within the brucite-like layer and the parameter "*c*" related to the total thickness of the brucite-like layer and the interlayer distance, have been evaluated by the least squares method (Table 1). As already stated, when series of LDHs containing two divalent cations or two trivalent cations in the layers are prepared, the Vegard's rule is followed and steady changes in the value of parameter "*a*" are observed with the chemical composition.[16] This is also the case for the copper cations substitution: the parameter "*a*" increases as the degree of substitution by Cu^{2+} is increased (Figure 2); the ionic radius of octahedral Ni^{2+} is 0.83 Å, whereas that of the octahedral Cu^{2+} is 0.87 Å.[17] While the value of parameter "*a*" is very sensitive to the nature of the layer cations (ionic radii), the value of parameter "*c*" strongly depends on the nature and orientation of the interlayer anions, therefore it cannot be observed a rule for the data from the seventh column of Table 1 because there is the same anion for all the LDHs and the small variations observed for "c" parameters are caused by the different degrees of hydratation.

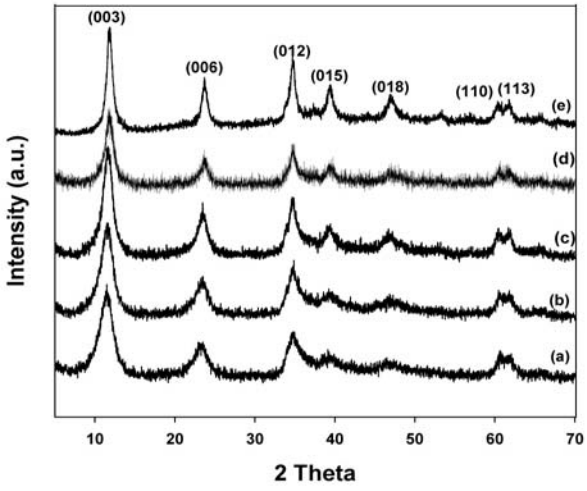

Fig. 1: Powder X-ray diffraction of LDHs: a. ZNCA10, b. ZNCA82, c. ZNCA55, d. ZNCA28, e. ZNCA01.

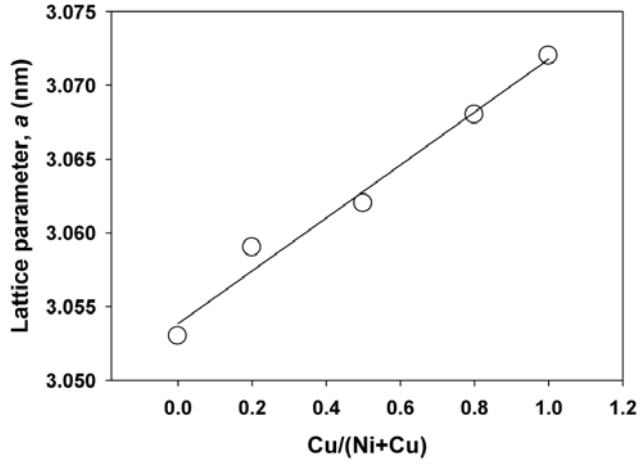

Fig. 2: LDH samples: unit cell parameter, *a* as a function of the Cu/(Ni+Cu) ratio

Table 1: Physical properties of non-calcined LDHs obtained from XRD and N_2 physisorption isotherms at –196 °C.

Sample	Atomic ratios*				*a*	*c*	$D_{(003)}$	$D_{(110)}$	S_{BET}	S_{ext}	V_t	APS_{BJH}
	Zn	Ni	Cu	Al	(Å)	(Å)	(nm)	(nm)	($m^2.g^{-1}$)	($m^2.g^{-1}$)	($cm^3.g^{-1}$)	(Å)
ZNCA**10**	1.0	**1.0**	**0.0**	1.0	3.053	22.60	4.5	10.7	37	32	0.31	333
ZNCA**82**	1.0	**0.8**	**0.2**	1.0	3.059	22.90	4.7	11.8	50	44	0.41	330
ZNCA**55**	1.0	**0.5**	**0.5**	1.0	3.062	23.01	6.2	11.8	70	61	0.47	272
ZNCA**28**	1.0	**0.2**	**0.8**	1.0	3.068	22.50	7.2	11.9	83	73	0.58	284
ZNCA**01**	1.0	**0.0**	**1.0**	1.0	3.072	22.38	9.5	14.5	86	76	0.75	349

* synthesis mixture; $a = 2d_{110}$; $c = 3d_{003}$; $D_{(003)}$ = crystallite size in *c* direction; $D_{(110)}$ = crystallite size in *a* direction; S_{ext} = external surface calculated from *t*-plot; V_t = total pore volume at $p/p_o \sim 0.99$; APS_{BJH} = average pore size determined according to the BJH method.

The values obtained for lattice parameters are in agreement with those previously reported in the literature for the carbonate-LDHs.[1]

The textural properties of LDHs were examined by N_2 physisorption. Figure 3 A shows the nitrogen adsorption–desorption isotherms for all the samples. According to IUPAC classification, the isotherms are of type IIb. [18] The hysteresis loop is of type H3, which is usually associated with the condensation-evaporation phenomena between aggregates of plate-like particles giving rise to slit-shaped pores.[19,20] As shown in Table 1, the external surface area is very close to the BET surface area. These values are in agreement with the literature since the diameter of nitrogen molecule is larger than the interlamellar space for carbonate containing layered double hydroxides, and therefore the pore volume measured corresponds mainly to the interparticle pores. The mesoporous structure of LDHs may arise from interparticle space; hence the characteristics (shape, size, distribution, etc.) of mesopores could be defined by the particle size and shape, and also by the particle interconnection patterns. Consequently, it is clear that the textural properties of these solids will finally depend on the morphological properties of the particles.[21,22] The corresponding pore size distribution plots (Figure 3, B) show a very large distribution between 10 and 2000 Å centered at ca. 300 Å.

Textural parameters provided by the corresponding isotherms such as BET surface areas, external surface areas, pore volume as well as average pores size are summarized in Table 1. According to physisorption data, the surface area and total pore volume increase with the amount of copper introduced in the brucite layer; these values range from 37 $m^2.g^{-1}$ (ZNCA10) to 86 $m^2.g^{-1}$ (ZNCA01) and from 0.31 $cm^3.g^{-1}$ (ZNCA10) to 0.75 $cm^3.g^{-1}$ (ZNCA01), respectively.

Figure 4 illustrates the TG curves together with the corresponding DTG curves for ZNCA01, ZNCA55, and ZNCA10 samples.

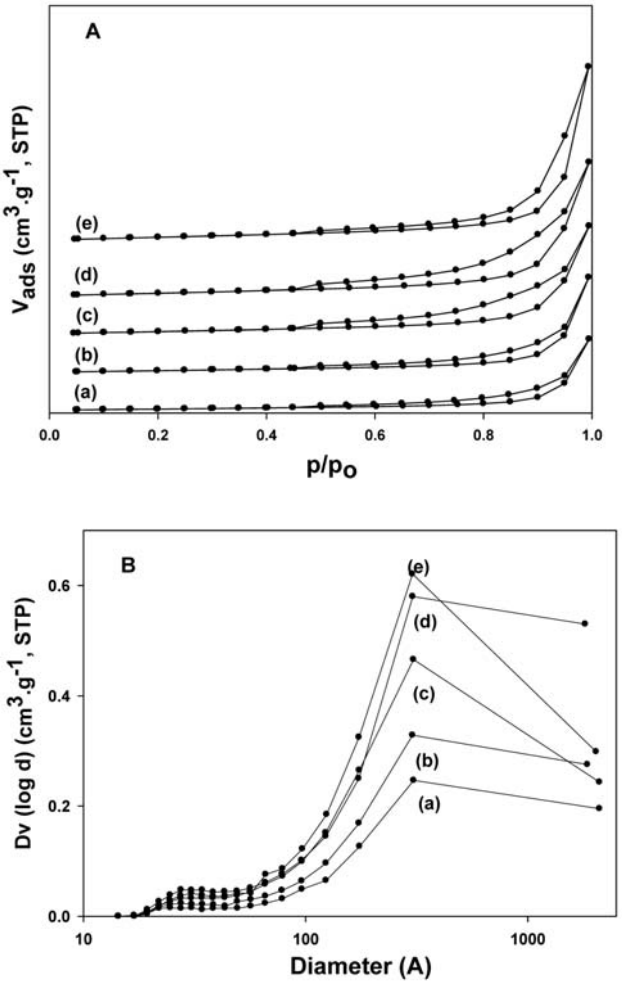

Fig. 3: Nitrogen adsorption-desorption isotherms (A) (the curves are shifted along the y-axis for clarity) and pore size distribution (B) for ZnNiCuAl-LDHs. a. ZNCA101, b. ZNCA82, c. ZNCA55, d. ZNCA28, e. ZNCA01. (STP = standard pressure and temperature)

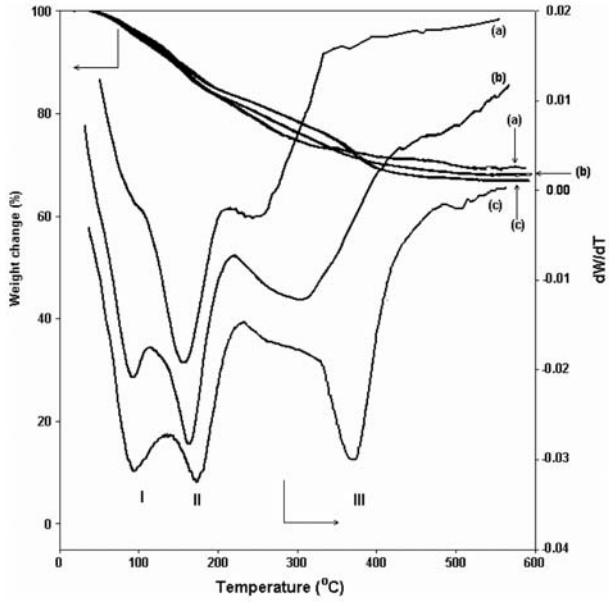

Fig. 4: TG/DTG profiles of: a. ZNCA01, b. ZNCA55, c. ZNCA10.

Three steps of weight loss between 30 and 400 °C were identified. The first weight loss with a maximum at ~ 100 °C corresponds to the removal of interlayer and weakly adsorbed water molecules and it is reversible. It is known that Cu ions incorporated into brucite layer strongly influence this stage of thermal decomposition of LDHs.[23] Thus, the higher amount of copper the lower is the amount of the physisorbed water. As seen in Figure 4, our results are in agreement with this, the amount of released water decreasing with the amount of copper in the brucite sheets. Also, the temperature at which the interla-

yer water is released is lowered for Cu containing LDHs. These results indicate that water molecules are not very tightly bonded to the LDH's layers when Cu is included in the brucite like layers. [23]

This weight loss was immediately followed by a second one with a maximum at 146 °C and a third one with a maximum at 230 °C which are attributed to the dehydroxylation of the layers and decomposition of intercalated carbonate anions, respectively. According to Cavani,[1] these two peaks are attributed to the loss of hydroxyl groups bound to Al cations (146 °C) and carbonate anions decomposition (230 °C).

Additional structural information were provided by infrared spectroscopy. Infrared spectra were recorded at room temperature and the results are shown in Figure 5. The infrared band at 3437 cm^{-1}, present in all the spectra, is attributed to the H-bonding stretching vibrations of the OH group in the brucite-like layer.[1] The band at 1635 cm^{-1} is assigned to the deformation mode of water molecules presented in the interlayer space.[24,25]

The wavenumber region ranging from 400 to1000 cm^{-1} contains some bands related to vibrations of the carbonate, and some related to cation-oxygen bond vibrations. The carbonate anion in a symmetric environment is characterized by a D3h planar symmetry, with three IR active absorpion bands at 1350–1380 cm^{-1} (ν_3), 850–880 cm^{-1} (ν_2) and 670–690 cm^{-1} (ν_4).[1] The spectra registered for our samples contain only a band at 1360 cm^{-1} assigned to ν_3 vibration.

Bands below 1000 cm^{-1} provide proof that the characteristic LDH network has been formed. They are due to stretching and deformation modes of M-O, M-O-M', and O-M-O moieties in the brucite-like layers, together with other modes of the carbonate anion.[26–28]

Further information on the status of the transition metal ions on the surface of the LDH samples were obtained by the DR-UV-VIS spectra displayed in Figure 6. Different bands were identified in these spectra. As Al^{3+} and Zn^{2+} have *d*0 and *d*10 configuration, respectively, all the bands recorded in UV-VIS region (205, 220, 242, 380, 414, 650, 740 and 770 nm) should be ascribed to the *d–d* transitions in the octahedrally coordinated Ni^{2+}, Cu^{2+} cations. Moreover, the bands at 205, and 220 nm could be also ascribed to $O^{2-} \rightarrow M^{n+}$ charge transfer.[2,29]

The intensity of the different bands increased as a function of the amount of Cu and Ni cations from the samples. Consequently, LDHs with higher amount of nickel (ZNCA55, ZNCA82 and ZNCA10) showed absorption in the UV range at 380 nm and in the VIS range at 414, 650 nm attributed to octahedral Ni^{2+}.[30] As nickel is replaced by copper, the band at 740 nm increases and it is slightly shifted to higher wavelength so that in the samples ZNCA28 and ZNCA01 only the band at 770 nm is identified in the spectra and it could be assigned to the Cu^{2+} ions in the distorted octahedron, which are located at the edge of the brucite-like layers. Indeed, this band completely disappeared in the spectrum of the ZNC28 after the catalytic test (spectrum not shown here). Instead of

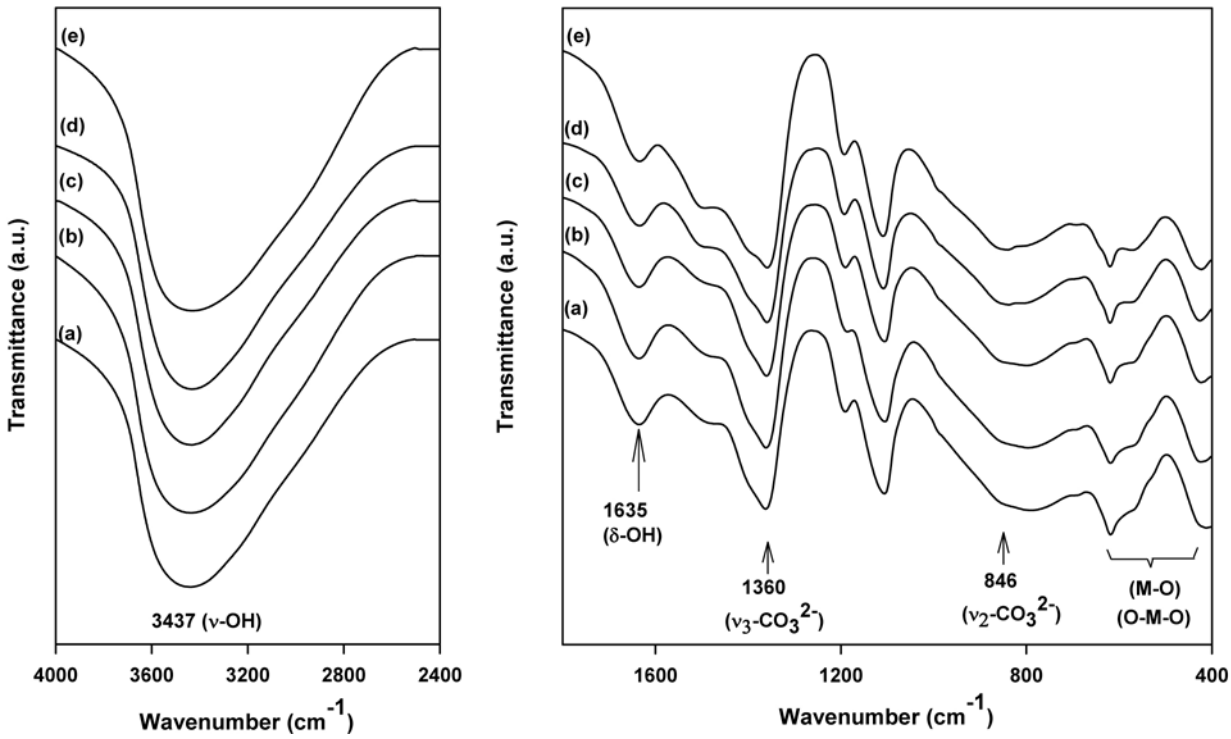

Fig. 5: FT-IR spectra of LDHs: (a) ZNCA10, (b) ZNCA82, (c) ZNCA55, (d) ZNCA28, (e) ZNCA01.

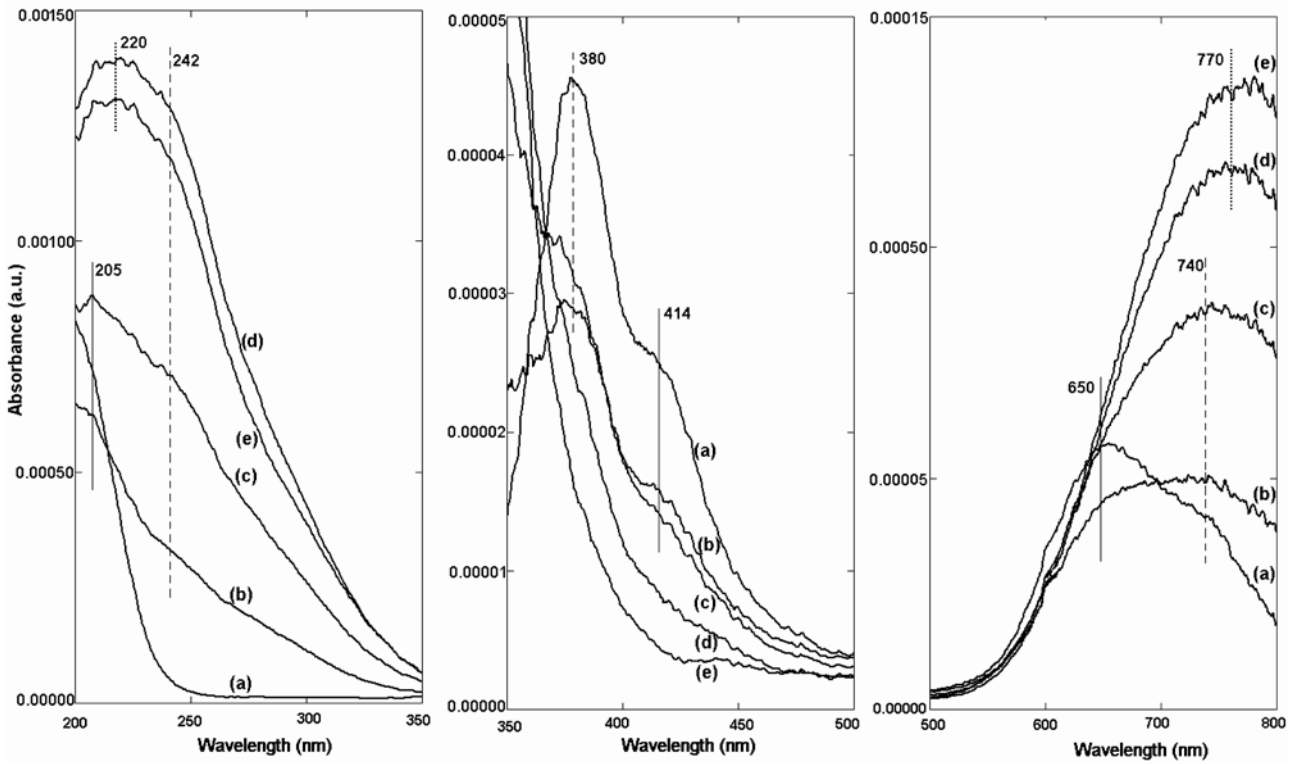

Fig. 6: DR-UV-VIS spectra of LDHs : (a) ZNCA10, (b) ZNCA82, (c) ZNCA55, (d) ZNCA28, (e) ZNCA01.

this, a new band at 600 nm was observed. According to the literature, Cu^{o} atoms absorb radiations at this wavelength.[31] Additionally, the band at 242 nm (octahedral Cu^{2+}) did not disappear after reduction by H_2 flow treatment for 2 h. The band at 380 nm did not suffer any change after the catalytic test suggesting that Ni^{2+} cations are not reduced at 150 °C. This result clearly suggests that only copper ions placed at the edges of the brucite-like layers and/or crystal defects are able to be reduced.[2]

3. 2. Catalytic Activity of LDH

For the first time, the catalytic hydrogenation of unsaturated carbonyl compounds in the presence of non-calcined LDHs is presented here. During activation process under H_2 stream at 150 °C, the solids preserve their hydrotalcite-like crystalline structure (not shown here).

Generally, the catalytic liquid phase hydrogenation of cinnamaldehyde proceeds via reaction pathways that involve hydrogenation of C=O and/or C=C groups (Scheme 1), the degree of the hydrogenation and the route depending on the activity and selectivity of the catalyst.

Cinnamaldehyde hydrogenation on non-calcined ZnNiCuAl-LDH with Ni/Cu = 2/8 molar ratio formed essentially hydrocinnamaldehyde (HCNA), cinnamyl alcohol (CNOL), and hydrocinnamyl alcohol (HCNOL); only traces of condensation products (~ 1–2%) were observed.

Figure 7 presents a typical time course of the hydro-

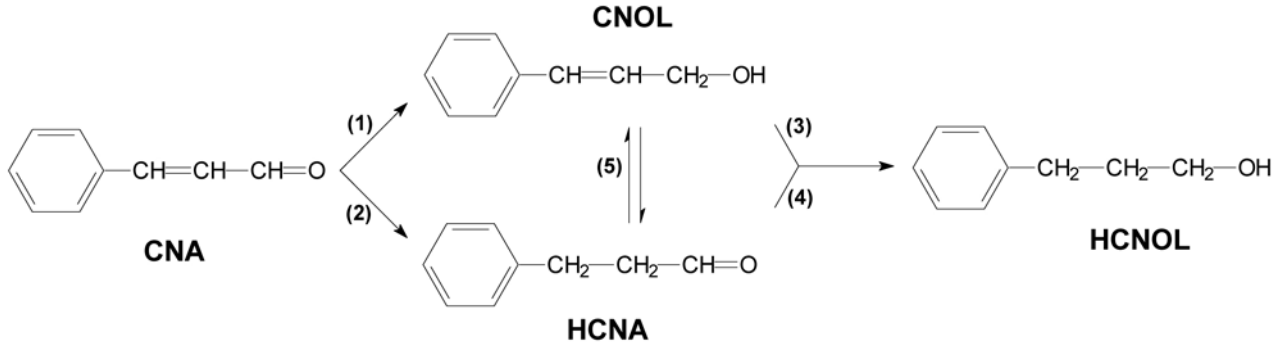

Scheme 1. Reaction pathways for CNA hydrogenation

genation of CNA over non-calcined ZNCA28 sample. As observed, CNA was completely consumed during 24 h of reaction, which means that the non-calcined but reduced LDH is an active hydrogenation catalyst. In the first 15 h of reaction, the hydrogenation carried out preferentially to C=C bond, with selectivity to HCNA of around ~ 60% for a conversion of ~ 40%, where conversion and selectivity were calculated according to following equations:

$$\%\ conversion = \frac{mole\ of\ hydrogenated\ CNA}{mole\ of\ total\ product} * 100$$

$$\%\ selectivity = \frac{mole\ of\ product\ CNA}{mole\ of\ hydrogenated\ CNA} * 100$$

The hydrogenation of C=O group was less active, a selectivity to CNOL of ~ 40% for a conversion of ~ 20% was noticed. At the end of the reaction, only HCNOL (~ 60%) and HCNA (~ 40%) were observed in the reaction mixture. These results indicate that the hydrogenation of CNA involves parallel and consecutive reaction as shown in Scheme 1.

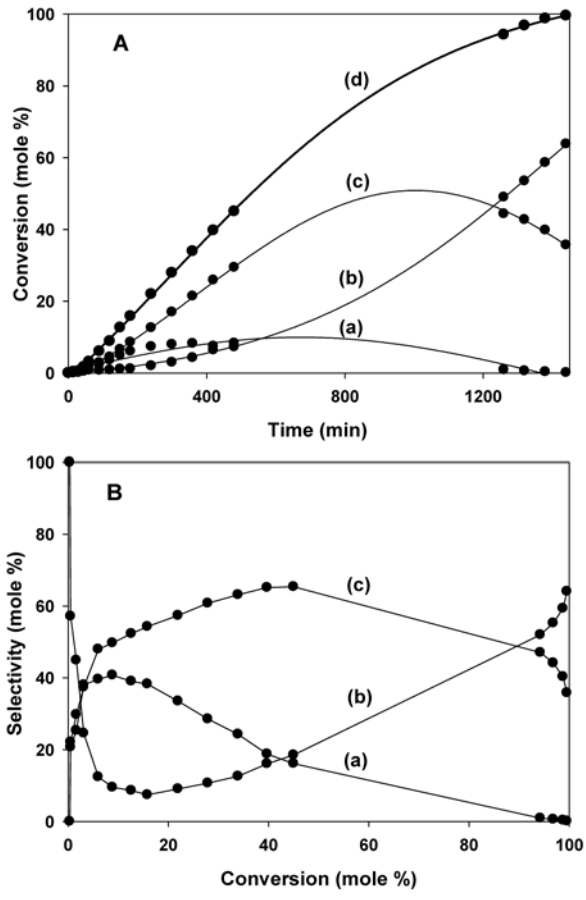

Fig. 7: Hydrogenation of CNA over non-calcined ZNCA28; T = 150 °C, catalyst mass = 0.264 g catalyst; CNA = 1 ml, solvent = propylene carbonate, (25 ml) stirring = 900 rpm; (a) – CNOL, (b) – HCNOL, (c) – HCNA; (d) – total conversion.

Previous studies showed that the selective hydrogenation to C=C or C=O bonds is depending on various factors among them the metal electron density, and C=O bond polarization by its interaction with cationic sites being the most important. [32,33–37]

The chemistry of the catalyst is also a key factor in directing the selectivity towards CNOL, knowing that usually, the hydrogenation at C=C group is thermodynamically favored.[38] Concerning Cu-based catalysts, it was reported that CNA adsorption on metal copper particles is expected to occur via π_{CC} and/or $d_{i-\pi}$ adsorption modes, both of them being influenced by the repulsive forces existing between copper *d* orbitals and the phenyl group of cinnamaldehyde.[32] Moreover, the catalytic results strongly suggest that CNA hydrogenation occurs via different reaction mechanisms depending on the composition and surface properties of the catalyst.[32,39] It was shown that CNOL formation rate is essentially increased on spinel Cu–Ni(Co)–Zn–Al catalysts compared to Cu/SiO_2 or binary Cu–Al samples because of the formation of surface Cu^o–M^{2+} dual sites (M^{2+} = Co, Ni, Zn). The reduction temperature used for the catalytic test in this work is low enough (150 °C) to avoid the reduction of Ni^{2+}. These cations, beside of Zn^{2+} and Al^{3+}, probably act as Lewis acids during the reaction activating the C=O functional group of CNA. The C=O bond thus activated is more easily hydrogenated by hydrogen atoms chemisorbed onto reduced copper. However, the electron density around copper could be probably increased by optimizing the catalyst composition, and it might cause a further improvement in the catalyst ability for selectively hydrogenating the C=O group of CNA.

Concerning particle size, its effect on the catalyst selectivity in hydrogenation of α,β-unsaturated aldehydes is a controversy. There are studies indicating no influence of the particle [36] while other articles claim that particle size is able to direct the selectivity of the catalyst due to the fact that the relative amounts of corners, edges and faces exposed to the reactants vary as function of the particle size.[8,40,41] The atoms in different crystallographic positions can have different catalytic properties, resulting in different selectivities and activities as a function of the particle size. Future studies on the catalytic activity of this series of catalysts will allow observing if there is some dependency between the particle size and the selectivity of the catalysts under study.

4. Conclusions

ZnNiCuAl LDHs were obtained by coprecipitation method with variable Ni/Cu ratios. Different techniques such as XRD, nitrogen physisoprtion at –196 °C, FT-IR, DR-UV-VIS and themogravimetry confirmed the specific lamellar structure of the resulted catalysts. Preliminary test in the liquid phase hydrogenation of trans-cinnamal-

dehyde on the non-calcined catalyst led to results which demonstrate that physico-chemical properties of layered double hydroxides are essential to achieve the improved product selectivity by optimizing their composition and particle size.

5. Acknowledgements

The authors gratefully acknowledge the financial support from the National Council of Romania under PNII-Idei Project No. 485/2009.

6. References

1. F. Cavani, F. Trifiró, A. Vaccari, *Catal. Today* **1991**, *11*, 173–301.
2. M. Crivello, C. Perez, E. Herrero, G. Ghione, S. Casuscelli, E. Rodriguez-Castellon, *Catal. Today* **2005**, *107–108*, 215–222.
3. F. Malherbe, C. Depege, C. Forano, J.P. Besse, M.P. Atkins, B. Sharma, S.R. Wade, *Appl. Clay Sci.* **1998**, *13*, 451–466.
4. K. Zhu, C. Liu, X. Ye, Y. Wu, *Appl. Catal. A: General* **1998**, *168*, 365–372.
5. A. Vaccari, *Catal. Today* **1998**, *41*, 53–71.
6. G. Szöllösi, M. Bartok, *J Mol. Catal A: Chem*. **1999**, *148*, 265–273.
7. B. M. Reddy, G. M. Kumar, I. Ganesh, A. Khan, *J. Mol. Catal A: Chem.* **2006**, *247*, 80–87.
8. F. Delbecq, P. Sautet, *J. Catal*. **1995**, *152*, 217–236.
9. M. Chatterjee, F. Y. Zhao, Y. Ikushim, *Catal. Lett.* **2002**, *82*, 141–144.
10. M. Shirai, T. Tanaka, M. Arai, *J. Mol. Catal. A: Chem.* **2001**, *168*, 99–103.
11. R. Hubaut, J. P. Bonelle, M. Daage, *J. Mol. Catal*. **1989**, *55*, 170–183.
12. R. Hubaut, M. Daage, J. P. Bonelle, *Appl. Catal*. **1986**, *22*, 231–241.
13. H. Noller, J. E. German, *J. Catal*. **1984**, *85*, 25–30.
14. G. J. Hutchings, F. King, I. P. Okoye, C. H. Rochester, *Catal. Lett.* **1994**, *23*, 127–133.
15. G. J. Hutchings, F. King, I. P. Okoye, C. H. Rochester, *Appl. Catal*. **1992**, *83*, L7–L13.
16. V. Rives, *Mater. Chem. Phys*. **2002**, *75*, 19–25.
17. www.webelements.com
18. F. Rouquerol, J. Rouquerol, K. Sing, Adsorption by Powders and Porous Solids: Principles, Methodology and Applications, Academic Press, London, **1999**, pp 365.
19. F. Malherbe, C. Forano, J-P. Besse, *Micropor. Mater.* **1997**, *10*, 67–84.
20. D. Francova, N. Tanchoux, C. Gerardin, P. Trens, F. Prinetto, G. Ghiotti, D. Tichit, B. Coq, *Microporous Mesoporous Mater*. **2007**, *99*, 118–125.
21. P. Benito, F.M. Labajos, J. Rocha, V. Rives, *Microporous Mesoporous Mater*. **2006**, *94*, 148–158.
22. E. M. Seftel, E. Popovici, M. Mertens, K. De Witte, G. Van Tendeloo, P. Cool, E.F. Vansant, *Microporous Mesoporous Mater*. **2008**, *113*, 296–304.
23. L. Chmielarz, P. Kustrowski, A. Rafalska-Łasocha, D. Majda, R. Dziembaj, *Appl. Catal. B: Environ.* **2002**, *35*, 195–210.
24. S. Kannan, V. Rives, H. Knözinger, *J. Solid State Chem*. **2004**, *177*, 319–331.
25. K. Parida, J. Das, *J. Mol. Catal. A: Chem.* **2000**, *151*, 185–192.
26. A. Monzón, E. Romeo, C. Royo, R. Trujillano, F. M. Labajos, V. Rives, *Appl. Catal. A.* **1999**, *185*, 53–63.
27. Z. Chang, D. G. Evans, X. Duan, C. Vial, J. Ghanbaja, V. Prevot, M. de Roy, C. Forano, *J. Solid State Chem*. **2005**, *178*, 2766–2777.
28. V. Rives, O. Prieto, A. Dubey, S. Kannan, *J. Catal*. **2003**, *220*, 161–171.
29. M. J. Holgado, V. Rives, M. S. San Román, *Appl. Catal A: General* **2001**, *214*, 219–228.
30. M. A. Zanjanchi, A. Ebrahimian, *Mater. Chem. Phys*. **2008**, *110*, 228–233.
31. Z. Sojka, F. Bozon-Verduraz, M. Che, in : G. Ertl, H. Knözinger, F. Schüth, J. Weitkamp (Eds.), Handbook of Heterogeneous Catalysis, 8 Volumes, 2nd Edition, Wiley-VCH Verlag GmbH& Co. KGaA, Weinheim, **2008**, pp. 1047.
32. A. J. Marchi, D. A. Gordo, A. F. Trasarti, C. R. Apesteguýa, *Appl. Catal. A: General* **2003**, *249*, 53–67.
33. M. Lashdaf, A. O. I. Krause, M. Lindblad, M. Tiitta, T. Venalainen, *Appl. Catal. A* **2003**, *241*, 65–75.
34. A. Giroir-Fendler, D. Richard, P. Gallezot, *Catal. Lett*. **1990**, *5*, 175–181.
35. S. Galvagno, G. Capannelli, G. Neri, A. Donato, R. Pietropaolo, *J. Mol. Catal*. **1991**, *64*, 237–246.
36. L. Mercadante, G. Neri, C. Milone, A. Donato, S. Galvagno, *J. Mol. Catal. A: Chem.* **1996**, *105*, 93–101.
37. J. Hajek, N. Kumar, V. Nieminen, P. Maki-Arvela, T. Salmi, D. Y. Murzin, L. Cerveny, *Chem. Eng. J.* **2004**, *103*, 35–43.
38. F. Coloma, A. Sepflveda-Escribano, J. L. G. Fierro, F. Rodriguez-Reinoso, *Appl. Catal. A: General* **1996**, *148*, 63–80.
39. M. Englisch, V. S. Ranade, J. A. Lercher, *J. Molec Catal. A: Chem*., **1997**, *121*, 69–80.
40. A. J. Plomp, H. Vuori, A. O. I. Krause, K. P. de Jong, J. H. Bitter, *Appl. Catal. A: General* **2008**, *351*, 9–15.
41. S. Galvagno, A. Donato, G. Neri, R. Pietropaolo, G. Capannelli, *J. Mol. Catal.* **1993**, *78*, 227–236.

Povzetek

Z metodo soobarjanja smo sintetizirali Zn/Ni/Cu/Al plastne dvojne hidrokside z različnimi razmerji Ni/Cu in s stalnima razmerjema Zn/Al in M^{2+}/M^{3+}. Namen dela je bil raziskati vpliv sestave, predvsem razmerja Ni/Cu, na fizikalne in katalitske lastnosti teh materialov. Rezultati rentgenske analize so pokazali, da so vzorci kristalinični in enofazni. Na osnovi spektroskopskih metod FT-IR in DR-UV-VIS sklepamo, da so tako nikljeve kot bakrove zvrsti prisotne v brucitu podobnih plasteh. Materiali so mezoporozni; specifična površina in volumen por, določena s fizikalno adsorpcijo dušika pri –196 °C, sta med 37 in 86 $m^2\ g^{-1}$ in 0.31 in 0.75 $cm^3\ g^{-1}$. Materiali izgubljajo maso med segrevanjem v treh stopnjah med 30 in 400 °C. Količina fizkalno vezane vode je odvisna od razmerja Ni/Cu. Preliminarni testi katalitske aktivnosti so pokazali nenavadne katalitske lastnosti nežganih vzorcev pri hidrogeniranju *trans*-cimetovega aldehida v tekoči fazi.